PION PRODUCTION FROM FEW NUCLEON SYSTEMS IN THE REGION OF THE Δ_{1232} RESONANCE.

by

KEITH MICHAEL FURUTANI

A THESIS
SUBMITTED TO THE
FACULTY OF GRADUATE STUDIES AND RESEARCH
IN PARTIAL FULFILLMENT OF THE REQUIREMENTS
FOR THE DEGREE OF DOCTOR OF PHILOSOPHY

IN
NUCLEAR PHYSICS

DEPARTMENT OF PHYSICS
THE UNIVERSITY OF MANITOBA
WINNIPEG, MANITOBA
DECEMBER 1991

ISBN 0-315-77966-7

PION PRODUCTION FROM FEW NUCLEON SYSTEMS IN THE REGION OF THE Δ_{1232} RESONANCE

BY

KEITH MICHAEL FURUTANI

A thesis submitted to the Faculty of Graduate Studies of the University of Manitoba in partial fulfillment of the requirements for the degree of

DOCTOR OF PHILOSOPHY

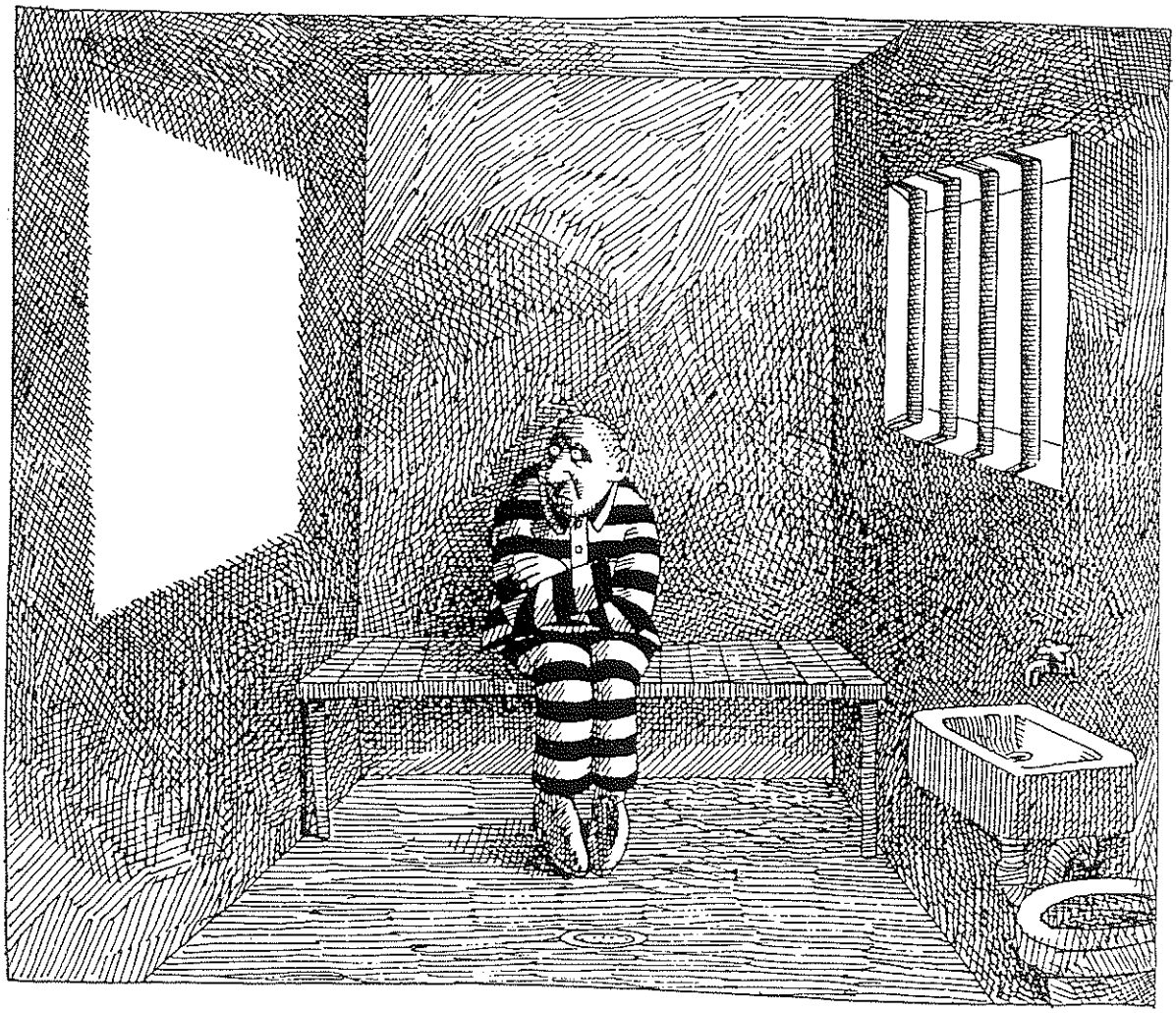

Abstract

Angular distributions of the differential cross sections and analyzing powers have been measured for the ^{3}He($\vec{p}$,π^+)^{4}He and ^{4}He($\vec{p}$,π^+)^{5}He reactions at proton bombarding energies between 240 and 507 MeV providing a comprehensive set of data spanning the region of the Δ_{1232} resonance.

For these experiments, the University of Manitoba/TRIUMF liquid ^{3}He target was extensively refurbished and modified for provision of stable and reliable operation. A Monte Carlo study of the TRIUMF Medium Resolution Spectrometer for detecting pions was performed to investigate the acceptance, solid angle, and pion decay length of the spectrometer. Furthermore, for the ^{5}He spectra, a final state interaction calculation was carried out which uses information from the n + α elastic phase shifts.

The results obtained are of very high quality and are compared with a recent microscopic (p,π^+) calculation and a phenomenological study based upon the pp $\rightarrow$ dπ^+ amplitudes.

Dedication

To my family

for giving me the courage to strive for such a goal

and

to Sandra

for the love and support to achieve it.

Acknowledgements

The content of this thesis is a refelection of the excellent guidance and supervision of a caring advisor, Dr. Willie Falk, whose attention to detail and insight into problems taught me more about physics than could be learned in any classroom or from any text. I am especially grateful that he had faith in an underdog student when others did not. I would also like to thank my committee for having the patience to hear all my questions and especially for their lucid answers.

There are three others whom also deserve special recognition. Two particularly close friends, Richard Y.H. Yeo and Alex Sekulovich, I would like to thank for the endless hours of discussion over many coffees and many beers of the salient points of getting through a graduate degree. My brother James, I must thank for having a generous heart to help me through the difficult times and for his bombastic nature to help me enjoy the good ones. Any accomplishments of mine are an influence of his positive spirit.

Acknowledgements are always very difficult to write since inevitably you leave someone out. That would be especially true in this case as I would never be able to acknowledge all the staff and friends that I have met and worked with over the past four years who had as much a part in my education as Dr. Bhakar's E & M course. I am indebted to them for their contributions to my outlook on physics and on life.

I would finally like to thank my high school physics teacher, Mr. K. Gerstmar, who possibly unknowingly, steered me into this crazy game which I have grown to love so much.

Contents

Abstract ii

Acknowledgements iii

Table of Contents iv

List of Figures ix

List of Tables xv

1 Introduction. 1

1.1 Elementary Pion Production 2

1.2 Nuclear Pion Production 5

1.2.1 Experimental 7

1.2.2 Theory 10

1.2.3 Negative Pion Production 16

1.2.4 Systematics of Observables 16

1.3 Few Nucleon Exclusive Pion Production 26

1.4 Summary 29

2 Experiments 30

2.1 Proton Beam 31

2.2 Target 34

2.2.1 Cryostat Design and Modifications 34

Helium Gas Handling System 34
Target Cell 36
2.2.2 Instrumentation 38
Vacuum 40
Helium Monitoring 41
Target Cell Monitoring 42
Computer 44
2.2.3 Operation 46
Cool Down 46
Maintenance 47
2.2.4 Tests for Liquid Helium Condensation 48
2.2.5 Beam Power Dissipation 53
2.2.6 Calibration 54
Volumes of Gas Handling System 54
Target Density 55
Target Planar Position 58
Target Rotation Position 60
2.3 Medium Resolution Spectrometer 61
2.3.1 Detectors and Coordinate Determination 63
Front End Chamber. 63
Drift Chambers. 63
2.3.2 Trigger and Data Acquisition 64
Trigger 64
Data Acquisition 65
2.3.3 MRS Transport 66
2.3.4 Event Reconstruction 71
Bend Plane Coordinates 72
Non Bend Plane Coordinates 78
Target Coordinates 79

2.3.5 Monte Carlo 80
Solid Angle 81
Pion Survival Fraction 83
Losses 86
Acceptances 86
2.4 Summary 89

3 Analysis 90
3.1 Data Extraction 90
3.1.1 Event Processing - LISA 90
3.1.2 Extraction of Peak Area for ^{4}He 93
3.1.3 Extraction of Peak Area for ^{5}He 93
Background Subtraction 96
Final State Interaction 101
Peak Integration and Normalization 113
3.2 Proton Beam Normalization 117
3.2.1 Proton Beam Normalization from SEM 117
3.2.2 Proton Beam Normalization from IBP 118
3.2.3 Comparison of Proton Beam Normalization from IBP and SEM 119
3.2.4 Beam Polarization from IBP 124
3.3 Efficiencies 125
3.3.1 Acquisition Live Time 126
3.3.2 Chamber Efficiencies 127
3.4 Acceptance 130
3.4.1 Focal Plane Acceptance 130
3.4.2 Target Acceptance 131
3.4.3 Test of Acceptance and Effective Length 133
3.5 Solid Angle 134
3.6 Results and Errors 136

3.6.1 Differential Cross Section Calculation 136
3.6.2 Analyzing Power Calculation 140
3.7 Summary 140

4 Results and Discussion **143**
4.1 Data 143
4.2 Systematics 146
4.3 Comparison to Previous Measurements 147
4.3.1 Comparison for ^{3}He($\vec{p}$,π^{+})^{4}He 150
4.3.2 Comparison to ^{3}H(n,π^{-})^{4}He 150
4.3.3 Comparison for ^{4}He($\vec{p}$,π^{+})^{5}He 159
4.4 Fit to Legendre Polynomials 162
4.5 Comparison to Elastic Data 167
4.6 Summary 168

5 Theory **169**
5.1 Early Calculations 169
5.1.1 Fearing DWIA Model 170
5.1.2 Gibbs and Hess Model 172
5.1.3 Cluster Model of Germond and Wilkin 173
5.2 Impulse Model 175
5.2.1 Description of Model 176
5.2.2 Calculation for ^{3,4}He($\vec{p}$,π^{+})^{4,5}He 178
5.3 Δ-Hole Model 181
5.4 ORCHID Model 182
5.4.1 Description of Model 182
5.4.2 Calculation for ^{3}He($\vec{p}$,π^{+})^{4}He 184
5.5 Discussion 189
5.6 Summary 189

6 Conclusions. **191**

Bibliography 194

A Data Acquisition Routine. 207

B Event Reconstruction Subroutine. 211

C Monte Carlo 217

D Phase Space 220

E Target Projection Calculation 225

F Solid Angle 230

G Data 236

List of Figures

1.1 Elementary pion production cross sections. 4

1.2 Momentum transfer for (p,π^+) reactions. 6

1.3 Energy spectrum from Dahlgren *et al.* showing quality of early pion production investigations. 8

1.4 Comparison of (d, p) and (p,π^+) stripping reactions. 10

1.5 Analyzing powers for the pp $\rightarrow$ dπ^+ reaction. 12

1.6 Analyzing power for ^{12}C($\vec{p}$,π^+)^{13}C from different ONM calculations at approximately 200 MeV. 13

1.7 Two Nucleon Model. 14

1.8 TNM calculation by Iqbal and Walker. 14

1.9 (p,π^+) total cross section dependence on target mass. 18

1.10 Kinematics for (p,π^+) reactions. 20

1.11 Momentum transfer for pp $\rightarrow$ dπ^+ and nuclear reactions. . . . 21

1.12 Kinematics for pp $\rightarrow$ dπ^+ and nuclear reactions. 22

1.13 Differential cross section versus the significant energy variable for the ^{12}C(p,π^+)^{13}C reaction and the pp $\rightarrow$ dπ^+ reaction. . . 23

1.14 Analyzing powers for some (p,π^+) reactions compared to the pp $\rightarrow$ dπ^+ reaction. 24

1.15 ORCHID calculation for ^{3}He($\vec{p}$,π^+)^{4}He at 178 and 198 MeV compared to the data of Kehayias *et al.* from IUCF. 27

1.16 Differential cross sections and analyzing powers at T_p = 800 MeV from Höistad *et al.* 28

2.1 TRIUMF beam line 4B. 32
2.2 BL4B In Beam Polarimeter. 33
2.3 Beam profile monitor 4BM7 showing Gaussian fit. 33
2.4 University of Manitoba/TRIUMF liquid ^{3}He cryostat. 35
2.5 Schematic of helium gas handling system. 37
2.6 Target cell general design. 38
2.7 Schematic of target cell. 39
2.8 Schematic of vacuum system. 41
2.9 Calibration of Top resistor. 43
2.10 Computer information page. 45
2.11 Target cell temperature response for cell under vacuum. . . . 49
2.12 Target cell temperature response for cell filled with liquid. . . 50
2.13 Schematic of the volumes for helium gas system. 51
2.14 Vapour pressure-temperature curves for ^{3,4}He. 51
2.15 Pressure-condensed volume calculation for ^{3}He. 53
2.16 Density of liquid ^{3}He at saturation. 56
2.17 Density of liquid ^{4}He at saturation. 56
2.18 Coordinates of target cell in 4BT2 scattering chamber 59
2.19 Calibration of rotation angle of cryostat. 61
2.20 Medium Resolution Spectrometer. 62
2.21 Cross sectional view of FEC showing position interpolation. . 64
2.22 Cross sectional view of VDC showing position interpolation. . 65
2.23 MRS trigger. 66
2.24 Scattering plane coordinate systems. 67
2.25 Coordinate systems of MRS. 67
2.26 Calculation of MRS optics to second order. 69
2.27 Coordinate systems of event reconstruction. 71
2.28 Focal Plane reconstruction from the VDC coordinates. 73
2.29 p_π/B versus XF from $pp \rightarrow d\pi^+$ scan. 75

2.30 Effect of kinematics on the focal plane resolution 76
2.31 Same as in Fig. 2.30 but with kinematic correction included. 77
2.32 (X,U) and (X,Y) coordinate systems of VDCs. 79
2.33 Calibration of the MRS quadrapole Hall probe. 82
2.34 Maximum muon lab angle for $\pi \rightarrow \mu\bar{\nu}_\mu$ decay. 84
2.35 $\pi \rightarrow \mu\bar{\nu}_\mu$ decay probability as a function of muon angle. . . . 85
2.36 Comparison of E413 and E564 pp $\rightarrow$ dπ^+ MRS focal plane acceptance scan with Monte Carlo results. 88
2.37 Comparison of E413 and E564 pp $\rightarrow$ dπ^+ MRS non bend plane acceptance scan with Monte Carlo results. 88

3.1 SPID spectrum, ESUM versus TTB. 92
3.2 Typical coordinate spectra for p ^{3}He $\rightarrow$ ^{4}He π^+. 94
3.3 Focal plane spectrum for p ^{3}He $\rightarrow$ ^{4}He π^+. 95
3.4 Focal plane spectrum for p ^{3}He $\rightarrow$ ^{4}He π^+ at back angles. . . 95
3.5 Energy level diagram for ^{5}He. 97
3.6 Focal plane spectrum for p ^{4}He $\rightarrow$ ^{5}He π^+. 98
3.7 Background pion momentum spectra. 99
3.8 Background pion spectra fit to Legendre polynomials. 100
3.9 Background pion spectrum. 100
3.10 p-wave phase shifts for α + n scattering. 101
3.11 The $p_{\frac{3}{2}}$ state n + α wave function. 103
3.12 The $p_{\frac{1}{2}}$ state n + α wave function. 103
3.13 The relativistic three particle phase space for p+$\alpha \rightarrow \pi^+$+n+α. 105
3.14 Comparison of $\psi(k,r)$ for k = 0.2 and 0.4 fm^{-1} to k = 0.1 fm^{-1} for $p_{\frac{3}{2}}$. 106
3.15 Comparison of $\psi(k,r)$ for k = 0.2 and 0.4 fm^{-1} to k = 0.1 fm^{-1} for $p_{\frac{1}{2}}$. 107
3.16 Comparison of $\psi_{3/2}(k,r)$ to $\psi_{1/2}(k,r)$ for k = 0.2 and 0.4 fm^{-1}. 108
3.17 Enhancement for π^+ + n + α. 109

3.18 Dependence of enhancement on r_1 and r_2. 110
3.19 Final state interaction for $\alpha + n + \pi^+$ spectrum. 112
3.20 Final state interaction for back angles. 114
3.21 Sensitivity of $\eta_{\rm fsi}$ on r_1 and r_2. 116
3.22 R(IBP/SEM) as a function of Run# for E413. 121
3.23 R(IBP/SEM) as a function of Run# for E564. 122
3.24 Position scan of 4B SEM at $T_p = 350$ MeV. 123
3.25 A_{N0} for pp elastic scattering. 124
3.26 A_{CH2}/A_H for BL4B In-Beam-Polarimeter. 125
3.27 Live times from BUSY/MASTER and PULSERS versus trigger rate. 126
3.28 Live times from PULSERS versus FEC rate. 128
3.29 Front End Chamber efficiency dependence on trigger rate. . . 129
3.30 Schematic of projection of active target volume onto MRS acceptance. 131
3.31 Projection of target profile onto MRS. 132
3.32 Comparison of ^{3}He($\vec{p}$,p)^{3}He analyzing powers. 141

4.1 Differential Cross Sections for the ^{3,4}He($\vec{p}$,π^+)^{4,5}He reactions. 144
4.2 Analyzing powers for the ^{3,4}He($\vec{p}$,π^+)^{4,5}He reactions. 145
4.3 Differential cross sections and analyzing powers at $T_p = 800$ MeV from Höistad *et al.* 146
4.4 Analyzing powers versus the three momentum transfer Q_{cm}. . 148
4.5 Analyzing powers versus the four momentum transfer t. . . . 149
4.6 Comparison of $T_p = 416$ MeV data with results from Tatischeff *et al.* 151
4.7 Comparison of σ(p,π^+) and σ(n,π^-) at 300 MeV. 154
4.8 Comparison of σ(p,π^+) and σ(n,π^-) at 416 MeV. 155
4.9 Comparison of σ(p,π^+) and σ(n,π^-) at 507 MeV. 156
4.10 Comparison of present and Källne *et al.* data. 158

4.11 Comparison of Tatischeff *et al.* data with Källne *et al.* results from Detailed Balance. 160
4.12 Coulomb effects from ORCHID calculation 161
4.13 Comparison of $^4He(\vec{p},\pi^+)^5He$ results. 162
4.14 $^4He(\vec{p},\pi^+)^5He$ at T_p=240 MeV fit to Legendre polynomials. . 165
4.15 $^3He(\vec{p},\pi^+)^4He$ at T_p = 300 MeV fit to Legendre polynomials. 166
4.16 Comparison of A_{N0} for the $^3He(\vec{p},\pi^+)^4He$ and $^3He(\vec{p},p)^3He$. . 167
4.17 Comparison of A_{N0} for the $^4He(\vec{p},\pi^+)^5He$ and $^4He(\vec{p},p)^4He$. . 168

5.1 Basic physical picture for phenomenological DWIA. 170
5.2 Calculation of $^3H(n,\pi^-)^4He$ by Alexander and Fearing. 172
5.3 Diagram for pion production in the model of Gibbs and Hess. 172
5.4 Calculation of $^3H(n,\pi^-)^4He$ by Gibbs and Hess. 174
5.5 Dynamics of cluster model of Germond and Wilkin. 175
5.6 Impulse model pion production mechanism in nuclei. 178
5.7 Impulse calculation for Differential Cross Sections. 179
5.8 Impulse calculation for Analyzing powers. 180
5.9 Δ-hole calculation by Sakamoto *et al.* 183
5.10 Two Nucleon mechanism of ORCHID model. 184
5.11 ORCHID calculation for $^3He(\vec{p},\pi^+)^4He$ at 178 and 198 MeV. 185
5.12 ORCHID calculation for $^3He(\vec{p},\pi^+)^4He$ at 300 MeV. 186
5.13 Decomposition of ORCHID calculation into contributions of one-nucleon, target-emission and projectile-emission mechanisms. 187
5.14 Effects of distortions in ORCHID calculation. 188

D.1 Calculation of the three particle phase space. 223
D.2 Same as in Fig. D.1 but plotted versus E_x. 224

E.1 Schematic of projection of active target volume onto MRS acceptance. 226

E.2 Definition of vectors for projection calculation. 227

F.1 The peak area versus solid angle for different FEC cuts. . . . 232
F.2 Solid angle versus Q/D determined with $pp \rightarrow d\pi^+$. 233
F.3 Q/D ratio versus run number for E413. 233
F.4 Solid angle versus Q/D ratio for E413. 234
F.5 Q/D ratio versus run number for E564. 235

List of Tables

1.1 Isospin cross section notation. 2

1.2 Isospin cross section reactions. 3

2.1 Experiments of this work. 30

2.2 Volumes of Helium gas handling system. 55

2.3 Comparison of elastic cross sections. 57

2.4 Position centres with respect to normal beam axis. 60

2.5 VDC's geometrical factors and nominal parameters for focal plane. 73

2.6 Typical losses due to absorption and multiple scattering determined by Monte Carlo. 87

3.1 Data word stream for MRS event. 92

3.2 Values for the potential for n + α scattering data. 102

3.3 FSI dependence on r_1 and r_2. 111

3.4 ^{4}He($\vec{p}$,π^+)^{5}He from LeBornec *et al.* 117

3.5 Calibration constants for BL4B SEM for E413 and E564. . . 118

3.6 IBP CH_2 areal target densities for E413 and E564. 119

3.7 Comparison of predicted and experimental R(IBP/SEM). . . 120

3.8 Acceptance tests with ^{3}He(p,π^+)^{4}He reaction. 134

3.9 Parameters used in cross section calculation. 137

3.10 Estimated or typical experimental errors. 138

3.11 Comparison of pp $\rightarrow$ dπ^+ cross sections with existing data. . 139

3.12 Comparison of ^{3}He($\vec{p}$,p)^{3}He analyzing powers. 141

4.1 Equivalent neutron energies for ^{4}He(π^-,n)^{3}H Detailed Balance. 153
4.2 Average RATIO of σ(p,π^+) to σ(n,π^-). 157

5.1 Bugg convention for pp $\rightarrow$ dπ^+ partial wave amplitudes. . . . 177

C.1 Monte Carlo elements. 217

F.1 Test of solid angle extraction with pp $\rightarrow$ dπ^+. 232

G.1 ^{3}He(p,π^+)^{4}He 300 MeV data. 237
G.2 ^{3}He(p,π^+)^{4}He 416 MeV data. 238
G.3 ^{3}He(p,π^+)^{4}He 507 MeV data. 239
G.4 ^{4}He(p,π^+)^{5}He ($\frac{3}{2}^-$) 240 MeV data. 240
G.5 ^{4}He(p,π^+)^{5}He ($\frac{3}{2}^-$) 300 MeV data. 241
G.6 ^{4}He(p,π^+)^{5}He ($\frac{3}{2}^-$) 400 MeV data. 242
G.7 ^{4}He(p,π^+)^{5}He ($\frac{3}{2}^-$) 500 MeV data. 243

Chapter 1

Introduction.

It has been fifty six years since Yukawa proposed the existence of a nuclear force quantum, the pion [Yuk35], and forty four years since its discovery [Lat+47]. In the intervening period to the present day, our knowledge of the Nucleon-Nucleon (NN) interaction has evolved to a point where extremely sophisticated potentials describe a vast amount of data. The NN data are conventionally parameterized in terms of partial waves, and it is at this point that experiment is compared to theory. The NN interaction is contemporarily described by boson exchange potentials (in which the pion is just one possible boson) which quantitatively describe the NN elastic phase shifts [Mac89] very well.

While these potentials describe very well the on-shell amplitudes (elastic scattering phase shifts), it is the off-shell scattering which is the test of the validity of the potential. The success of the description of NN elastic scattering is therefore naturally extended to a description of the inelastic channel, NN $\rightarrow$ NNπ. These reactions are less understood and tested, primarily because now the pion is allowed to carry away some of the momentum and energy and hence one is probing a much more extensive region of phase space than in the elastic case. Furthermore, there are now three bodies in

Isospin of two nucleons		Total
T_i	T_f	cross section
1	0	σ_{10}
0	1	σ_{01}
1	1	σ_{11}
0	0	forbidden

Table 1.1: Isospin cross section notation.

the final state so that the theoretical computations are more difficult than for the two body case. The contemporary NN $\rightarrow$ NNπ theories are still in the spirit of the boson exchange potentials, but with diagrams which allow an inelastic pion production channel [DKS87]. Such theories are still in the early stages of testing and development.

1.1 Elementary Pion Production

The elementary NN $\rightarrow$ NNπ process is comprised of several possible reactions (for example: pp $\rightarrow$ npπ^+, pp $\rightarrow$ ppπ^0 and np $\rightarrow$ ppπ^-). A simple classification results by considering the isospin basis. In the isospin basis there are only four reactions. These are denoted by the isospin of the two nucleons in the incident channel, T_i, and the outgoing channel, T_f [GW54] (see Table 1.1). Note that of the four only three are allowed, since the isospin of the pion is one.

The possible elementary pion production reactions and their relation to the isospin cross sections are shown in Table 1.2. Note that for the case of pp $\rightarrow$ npπ^+ (σ_{10}) there is the possibility of the np system forming a bound

Reaction	Cross section
$pp \rightarrow d\pi^+$	σ_{10}^{d}
$pp \rightarrow np\pi^+$	σ_{10}^{np}
$pp \rightarrow pp\pi^0$	σ_{11}
$np \rightarrow d\pi^0$	$\frac{1}{2}\sigma_{10}^{d}$
$np \rightarrow np\pi^0$	$\frac{1}{2}\sigma_{10}^{np} + \frac{1}{2}\sigma_{01}$
$np \rightarrow nn\pi^+$	$\frac{1}{2}\sigma_{11} + \frac{1}{2}\sigma_{01}$
$np \rightarrow pp\pi^-$	$\frac{1}{2}\sigma_{11} + \frac{1}{2}\sigma_{01}$

Table 1.2: Isospin cross section reactions.

state deuteron. Therefore, one usually makes the further distinction between the bound and unbound case, σ_{10}^{d} and σ_{10}^{np} respectively.

Using the available data the isospin cross sections may be determined and these are shown in Fig. 1.1 (from Ref. [VA82]). Note that the low energy pion production cross section is described mostly by σ_{10}^{d} (that is the $pp \rightarrow d\pi^+$ reaction).

The description of elastic and inelastic processes from nuclei (both nucleon-nucleon scattering and pion production) is often formulated from the point of view of the elementary NN processes. However, one now must consider the field of the nucleus and this is most often described in an averaged way by an optical potential. The technique is usually performed by fitting the optical potential parameters to the case of elastic scattering at or near an equivalent energy for the process of interest. As an example, in the case of a stripping reaction, A(d,p)A+1, the analysis is usually done in a simple Born Approximation (with plane waves, a PWBA, where the field of the nucleus is ignored, or with distorted waves from an optical potential, a DWBA). A

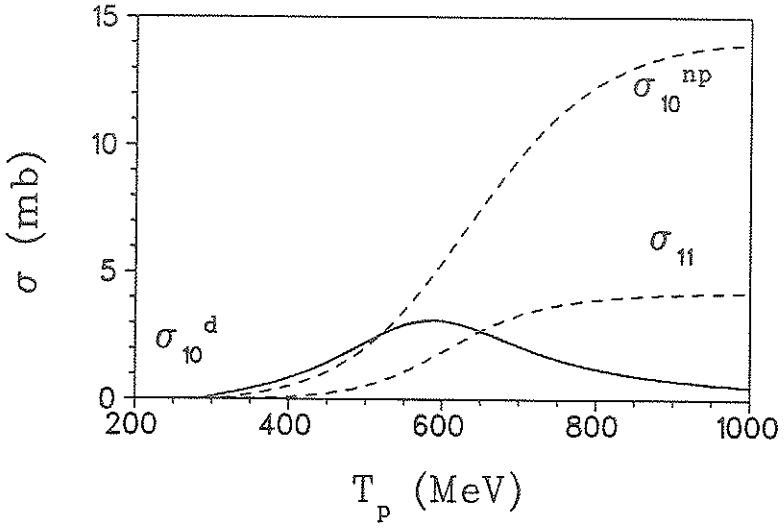

Figure 1.1: Elementary pion production cross sections.

method which is commonly used in the analysis of nucleon-nucleus elastic scattering is to include the information from the elementary processes (for example NN→NN) often obtained from the phase shifts. Such calculations are called Impulse Approximations (PWIA for plane waves and DWIA for distorted waves). A less common and much more difficult approach is to calculate the reaction mechanism using, for example, a boson exchange potential. The motivation for such calculations is to include the higher order processes explicitly rather than in an averaged way from an optical potential and in so doing investigate detailed points of the reaction mechanism. Such microscopic calculations are usually difficult and therefore are not as prevalent as the DWBA or DWIA calculations.

The reactions studied in this thesis are for few body nuclei (A=3,4) of the general A(p,π^+)A+1 reaction. These reactions may be studied theoretically in the context of a DWBA analysis (similar to those done for, say, (d,p)

stripping reactions) or with a full microscopic calculation. Examining these reactions from the point of view of the fundamental $NN \rightarrow NN\pi$ processes is also a useful approach, for example in a PWIA or DWIA calculation. These facets of A(p,π^+)A+1 reactions and the experiments performed to investigate them will now be discussed.

1.2 Nuclear Pion Production

Exclusive proton induced nuclear pion production is the study of reactions like A(p,π)A+1, where the residual A+1 nucleus is left in a well defined nuclear state. Due to the large mass difference between the incident proton and outgoing pion, there is a large momentum transfer imparted to the recoil nucleus. The momentum transfer (specifically the three momentum transfer) is defined in the following way.

$$\vec{q} = \vec{p}_f - \vec{p}_i \tag{1.1}$$

$$Q_{cm} = |\vec{q}| = \sqrt{p_i^2 + p_f^2 - 2p_i p_f \cos\theta_{cm}} \tag{1.2}$$

Even at threshold, the momentum transfer is large compared to the nuclear Fermi momentum (about 270 MeV/c). As an illustration, the momentum transfer versus the proton bombarding energy for the ^{3}He(p,π^+)^{4}He and the ^{40}Ca(p,π^+)^{41}Ca reactions is shown in Fig. 1.2.

It was this large momentum transfer which incited activity in the research of this reaction. It was hoped that using a simple reaction mechanism, similar to that for (d,p) stripping reactions studies, much could be learned about the high momentum components of nuclear wave functions. It was found, however, that such a simple picture did not explain the data adequately. Such ambiguities motivated detailed investigations of the reaction mechanism and also the limits of pion optical potentials. Continued uncertainty inspired

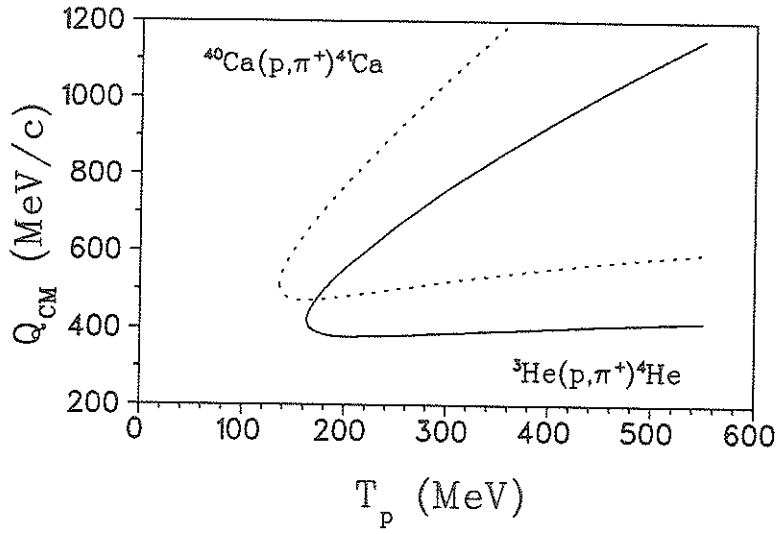

Figure 1.2: Momentum transfer for (p,π^+) reactions. The lower arm corresponds to Q_{cm} for 0° and the upper arm for 180°. (the solid line is for ^{3}He(p,π^+)^{4}He and the dotted line for ^{40}Ca(p,π^+)^{41}Ca).

more effort in both theoretical and experimental investigations. While the A(p,π^+)A+1 reaction has been a very difficult reaction to study theoretically, it has also shown to be a very sensitive proving ground for current nuclear reaction theories.

1.2.1 Experimental

The early work of nuclear pion production was carried out at only selected energies and angles. An example is the study of the ^{12,13}C(p,π^+)^{13,14}C and ^{14}N(p,π^+)^{15}N reactions at $T_p = 600$ MeV and $\theta = 0°$ done at CERN [Dom+70] over 20 years ago. This work was followed shortly by work at Uppsala [DHG71] where both positive and negative pion production on a large variety of targets was extensively studied (see for example Refs. [Dah+73a], [Dah+73b] and [Dah+73c]). All the work was carried out near threshold (185 MeV) and with non-polarized beams but is generally considered to be the pioneering work on nuclear pion production. As an example of the quality of these early works, an energy spectrum for ^{12}C(p,π^+)^{13}C from Ref. [DHG71] is shown in Fig. 1.3.

The earliest work of nuclear pion production involving measurements of polarization as well as differential cross section is that of Heer *et al.* [HRT58]. They investigated pion production from C and Al at 209 MeV, but at only a few angles. The polarized beam was generated in the standard manner of that time, namely via a double scattering experiment. The authors noted that such a measurement is extremely time consuming and therefore similar measurements were not performed. With the advent of the intense polarized proton beams, spin observables (notably the analyzing powers) then became additional observables of investigation. In the Ann Arbor [KS78] convention

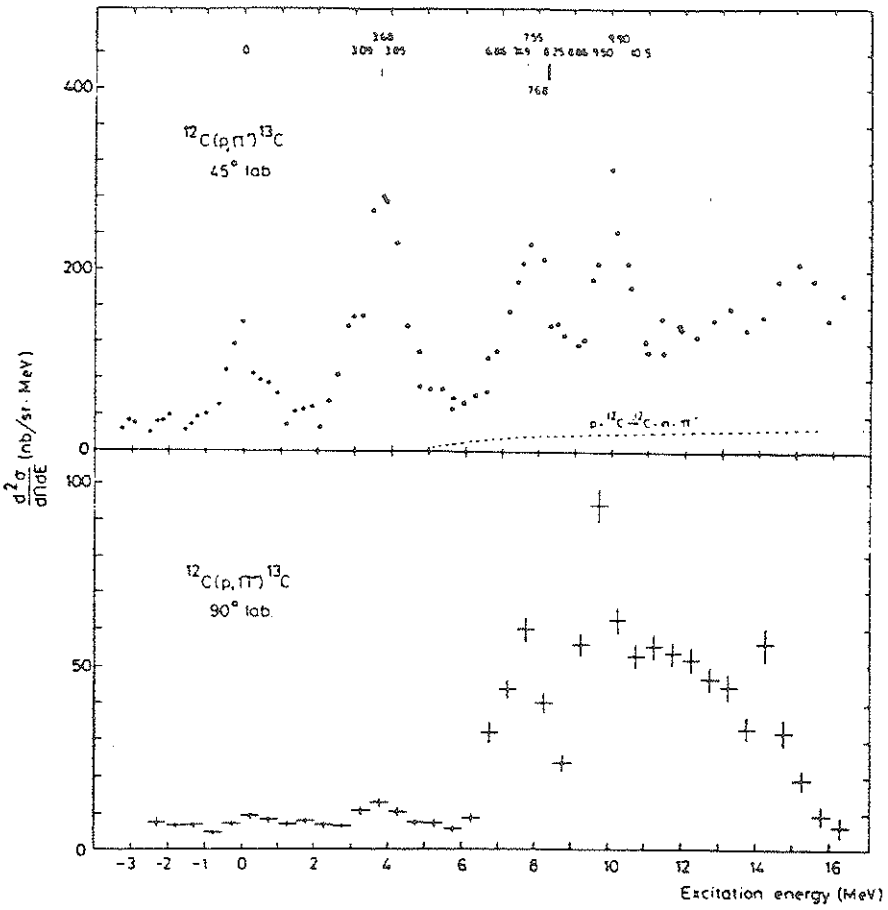

Figure 1.3: Energy spectrum from Dahlgren *et al.* showing quality of early pion production investigations.

the analyzing power is defined as

$$A_{N0} = \frac{1}{P} \frac{d\sigma(\uparrow)/d\Omega - d\sigma(\downarrow)/d\Omega}{d\sigma(\uparrow)/d\Omega + d\sigma(\downarrow)/d\Omega} \tag{1.3}$$

where P is the proton beam polarization. The subscript N indicates that the beam is polarized normal to the scattering plane and the subscript 0 indicates the target is unpolarized. The arrows indicate the direction of the polarization of the incident beam, i.e. up or down, with respect to the scattering plane (for example $d\sigma(\uparrow)/d\Omega$ is then the differential cross section for polarized-up protons). In the older Madison convention [BH71] the analyzing power is notated A_y. One should note that, by definition, the range of the analyzing power is between $+1$ and -1 and that it must be zero, by symmetry, for scattering angles of 0° and 180° .

Measurements of the analyzing power for a variety of nuclei near threshold were performed at the Indiana University Cyclotron Facility (IUCF) [Sjo+81] and at TRIUMF in Vancouver, Canada [Aul+78]. The analyzing power was found to be rich in structure and has, since then proven to be the point of greatest difficulty when comparing theory with data. In some nuclei, where the differential cross section may display only little variation with energy, the analyzing power may exhibit strong variation with energy. The analyzing power thus becomes a very important observable when studying (p,π^+) reactions.

As an indication of the amount of interest in these reactions generated by the research of the 1970's is the number of review articles of this field of research (see Refs. [Hoi79], [MM79] and [Fea81]). These reviews are excellent surveys of the data of that period and many of the conclusions and questions raised are still applicable today. Since the (p,π^+) conference in Indiana in 1981 [Ben82], many experiments have been performed and are usually of very high quality stressing the importance of polarization measurements.

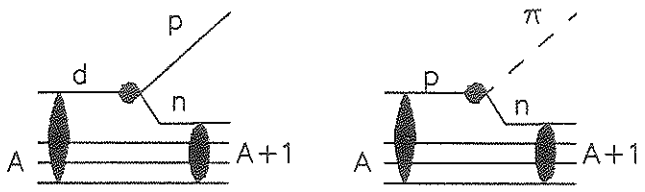

Figure 1.4: Comparison of (d, p) and (p,π^+) stripping reactions.

Such high quality data have inspired a great deal of theoretical activity as well, which will be presented in the following section.

1.2.2 Theory

In the initial investigations it was hoped that A(p,π^+)A+1 reactions would provide information about the high momentum components of nuclear wave functions. In the context of Direct Reaction theory one can make the obvious comparison between (d,p) and (p,π^+) reactions, as shown in Fig 1.4. It is therefore not difficult to see why these reactions were originally studied in the so called One Nucleon Model (ONM) or pionic stripping process analogous to a DWBA formalism used for (d,p) reaction studies.

As one might expect, the calculations were found to be very sensitive to optical model wave functions. Examples of DWBA calculations can be found in the work of Tsangarides [Tsa79]. His calculations were applied to many nuclei near threshold. In light of the comparison between (d,p) and (p,π^+) reactions, investigations of A(d,p)A+1 and A(p,π^+)A+1 were done at similar momentum transfers for several nuclei and the DWBA analyses per-